MAPAN-JOURNAL ,
Publisher: METROLOGY SOC INDIA ,
NPL PREMISES,
Address: DR K S KRISHNAN MARG, NEW DELHI,
INDIA, 110 012
ISSN / eISSN:0970-3950 / 0974-9853
Volume 25-Issue 1-(2025)

Research and Application of a Posture Correction System for Erhu Performance Based on Wearable and Body Sensing Technologies

Yubo Wang

Zhuhai University of Science and Technology, Zhuhai， 519000, China

Email ：134114164yubo@sina.cn

Abstrac

In the rapid development of science and technology, wearable technology devices, as the focus of scientific research in the new era, play an important role in the recognition and monitoring of human limb movements. As a traditional Chinese stringed instrument, the erhu itself has a profound historical and cultural heritage and unique artistic charm, and has become an indispensable part of the Chinese musical instrument family after thousands of years of development and innovation in China. Under the guidance of modern science and technology, the use of wearable and body sensing technology to accurately identify and correct the posture of erhu performers can not only improve the technical level of human posture recognition and monitoring, but also obtain more data and information to provide a reference for posture correction. Therefore, this paper mainly studies the Erhu performance posture correction system based on wearable and body sensing technology, and conducts performance verification analysis in combination with the practical experimental environment.

Keywords: wearable; body sensor technology; Erhu; Postural correction
AMS 2020 codes: 00000

†Yubo Wang.
Email address: wangyubo1357@outlook.com

ISSN 2xxxx-xxxx
DOI: xx.xxxx/AMANS.xxxx.xx.xxx

1 Gait correction system based on wearable sensing and haptic feedback

The gait correction system based on wearable sensing and haptic feedback studied in this paper is designed and optimized by using wearable sensing and haptic feedback after understanding the structure of the traditional gait correction system [1]. On the one hand, the feedback device will be installed in various parts of the user, and the collected sensor information will be transmitted to the data processing device, and after receiving, the feedback instruction of the data processing device will be executed; On the other hand, the data processing device calculates and analyzes the human gait parameters provided by the sensor information, compares the relevant parameters with the ideal parameters, and derives the feedback parameters, and then generates feedback instructions according to the parameters and sends them to the sensing feedback device to effectively correct the user's gait [2]. Combined with the system structure diagram shown in Figure 1 below, the overall design is more scientific and simple, and the sensing feedback device includes a first wireless module, a sensor, a first CPU, and a vibrator [3]. Wherein, the first wireless module can transmit sensor information to a data processing device and a receiving data processing device, and obtains feedback instructions; The first CPU can be used to obtain sensor information, transmit it to the first wireless module, and effectively control the vibrator in combination with feedback instructions; The vibrator can provide vibrating feedback in combination with feedback commands, reminding the user to adjust the corresponding gait [4]. The data processing device comprises a second wireless module, a second CPU, a display module, a Bluetooth module, a memory card and a USB interface. These contents will be connected to the second CPU, and the second CPU will calculate the gait parameters of the human body according to the sensor information, obtain feedback parameters after comparing and analyzing the experimental parameters and the ideal parameters, and generate feedback instructions thereby. The Bluetooth module will transmit the human gait parameters to the mobile phone client and receive control instructions, the memory card can store the information parameters of the sensor, and the USB interface is mainly used to send sensor information and feedback parameters to the computer client, and the client user can get the corresponding control instructions [5].

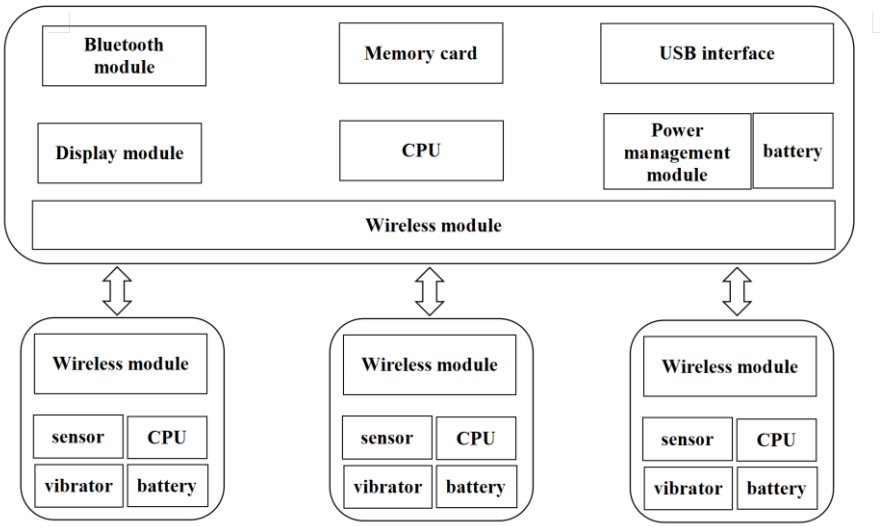

Figure 1 System architecture

2 Multi-feature fusion algorithm based on rotation angle

2.1 Design the framework

In this paper, a feature fusion algorithm with rotation angle is proposed in the feature extraction and selection stage, and the actual operation process is shown in Figure 2 below.

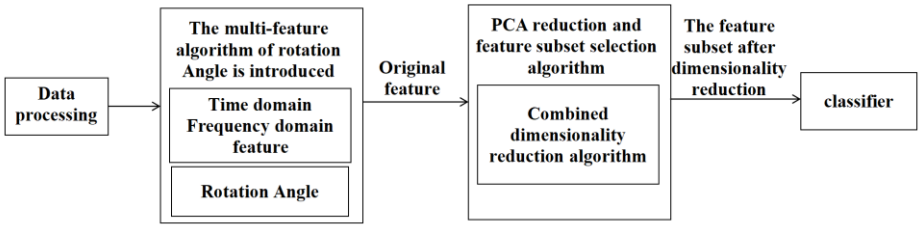

Figure2 Flow chart of multi-feature fusion algorithm

Combined with the analysis of the above figure, it can be seen that on the basis of clarifying the traditional time domain and frequency domain, the effective reaction action will change in three-dimensional space by introducing the basic information of rotation angle. During feature selection and extraction, the algorithm combining feature set selection algorithm and principal component analysis can not only ensure the dimension reduction, but also obtain more complete feature information [6]. The sensors of the research system need to be worn by the experimenter on the lower back, so as to collect and identify various movement information, and use Matlab software to professionally process it. For example, if the experimenter changes the action while the original position is shifted, it can be found that the acceleration and angular velocity information of the two actions of sitting down and lying down to sleep are similar, and both are non-periodic actions. When the experimenters walked straight forward and ran forward on flat ground, the movement changes of the two showed the characteristics of periodicity, and the movement changes during running were significantly larger than those when walking, but they could not be effectively distinguished by looking at the waveform changes alone. Although there are periodic characteristics, the data of the experimenter when going upstairs and bending over, but the spirometer data has a large difference, there will be large fluctuations when bending over, the ripples are very obvious, and the state when going up and down the stairs and walking is relatively similar, if only based on the relevant information of acceleration and angular velocity, it is difficult to accurately distinguish.

2.2 Introduce the rotation angle

Since the acceleration and angular velocity information cannot be used to accurately identify the action characteristics of the erhu performance pose, this paper studies and collects 8 basic actions, and after mastering the time-domain eigenvalues of the three-axis acceleration values of each action, the rotation angle is introduced to construct a multi-feature fusion algorithm.In the process of data

processing, all data information is reduced to a dimensionality, and the actual representation vector is

$$x = [x_1, x_2, \cdots, x_N]^r \tag{1}$$

The basic feature formula is shown in the following steps:

First, statistical characteristics. When studying statistical features, the maximum value, minimum value, variance, and average value are usually used in the time domain feature, and can often be used in acceleration information recognition, and the specific formula is as follows:

$$C = \sum_{i=1}^{n} \frac{X_i}{n}, \frac{\sum_{i=1}^{n} \left(X - \bar{X}\right)^2}{n}, min(X_i), max(X_i) \tag{2}$$

In the above formula, n represents the number of samples and X represents the first eigenvector, which represents the average value of the data.X_i

Second, peaks. When detecting the step size, the peak value is usually used, which can be directly presented using the acceleration data, and the specific formula is as follows:

$$\mathrm{b}k = \frac{\frac{1}{N}\sum_{i=1}^{N}\left(x_i - \bar{x}\right)^4}{\left(\frac{1}{N}\sum_{i=1}^{N}\left(x_i - \bar{x}\right)^2\right)^2} - 3 \tag{3}$$

In the above formula, bk represents the peak value of the sequence, N represents the number of samples, and x_i represents the value of the ith measurement, which represents the$x_i$calculated average value.

Third, the short-term Fourier transform. In the frequency domain, the Fourier transform is usually used, which is mainly used in the frequency component of the signal, and can effectively identify periodic actions [7]. In the long-term signal, because it will shift from the time domain and the frequency domain, part of the signal will be lost at this time, so it is not suitable for non-stationary signal analysis, and the short-time Fourier transform can be used to analyze the windowed signal, the specific formula is as follows:

$$STFT(t, f) = \int_{-\infty}^{\infty} x(\tau) h(\tau - t) e^{-j2\pi f \tau} d\tau \tag{4}$$

In the above formula, it refers to the window function of the analysis.$h(\tau - t)$

Fourth, skewness. Skewness measures the symmetry of the analyzed series, and if it is positive, the dispersion on the right side of the average value of the sample is higher than that on the left; If it is

negative, then the result is the opposite, and the actual calculation formula is as follows:

$$sk = \frac{\frac{1}{N}\sum_{i=1}^{N}\left(x_i - \bar{x}\right)^3}{\left(\frac{1}{N}\sum_{i=1}^{N}\left(x_i - \bar{x}\right)^2\right)^{3/2}} \tag{5}$$

Fifth, standard deviation. The standard deviation is used to measure the stability of the analysis data as follows:

$$X_{std} = \sqrt{\frac{1}{n}\cdot\sum_{i=1}^{n}\left(x_i - \bar{x}\right)^2} \tag{6}$$

Sixth, the correlation coefficient. The correlation coefficient represents the correlation of variables on two axes, and the data on each axis are different, which is an effective method for accurately judging the main characteristics of different actions, as shown below:

$$r(X,Y) = \frac{\sum_{i=1}^{N}\left(x_i - \bar{x}\right)\left(y_i - \bar{y}\right)}{\sqrt{\sum_{i=1}^{N}\left(x_i - \bar{x}\right)^2\sum_{i=1}^{N}\left(y_i - \bar{y}\right)^2}} \tag{7}$$

According to the research results of angular velocity-sensitive MEMS in recent years, this type of sensor is mainly used in the healthcare and fitness industries, and some scholars have used sensor technology to improve user authentication methods [8]. With the continuous development of artificial intelligence technology theories such as unmanned aerial vehicles, attitude angle calculation has become an important content in the field of pattern recognition, which is usually used in navigation systems, and this study integrates the information of attitude angle on this basis [12]. Although the accuracy of the triaxial acceleration, triaxial angular velocity, and magnetic field strength obtained by inertial sensors is steadily improving, the attitude angle cannot be directly estimated, and the common algorithms include direct integration, vector observation, and directional filtering algorithms, among which the calculation of the direct integration method is simpler [10]. At the same time, the systematic study introduces the information features of the rotation angle according to the angular velocity signal, which helps researchers to accurately judge the movement state of the erhu experimenter in three-dimensional space [12]. For example, the sagittal plane change of the experimenter's bending motion is defined as follows:

$$\theta(t) = \int_0^t \omega(\tau)d\tau + \theta_0 \tag{8}$$

In the above formula, it represents the angle of rotation, the angle at rest, and the angular velocity obtained by acquisition. In order to accurately judge the Euler angle, the noun of the angle of rotation is used to explain the angle of rotation of angular velocity in three axes.

2.3 Feature extraction

After the data preprocessing is completed, the multi-feature fusion process is carried out according to the flow chart shown in Figure 3 according to the obtained corresponding action feature values, and after the data filtering and window operation are completed, the window length is set to 4 seconds, the adjacent window is set to 50% overlap rate, and the corresponding window contains action information as shown in Table 1 below:

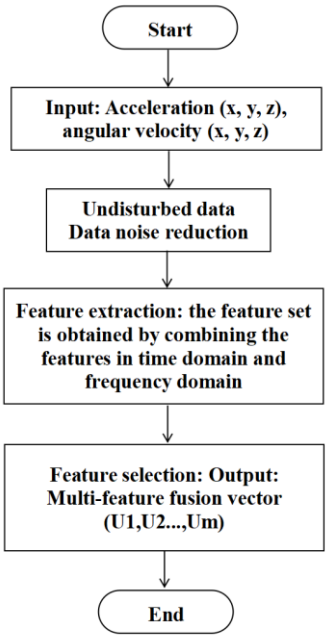

Figure 3 Flow chart of the multi-feature fusion algorithm

Table 1 Feature collection information

eature Type	Feature ID	Feature Description
	1-6	Mean
	7-12	Variance
	13-18	Skewness
	19-24	Peak Value
Time Domain	25-30	Maximum Value
	31-36	Minimum Value
	37-42	Standard Deviation
	43-48	Correlation Coefficient

Frequency Domain	49-54	Fourier Transform
	55-57	Mean Rotation Angle

The obtained features are formed into eigenvectors, and all eigenvectors are normalized to [0,1] intervals, as follows:

$$y_i = \frac{x_i - x_{min}}{x_{max} - x_{min}} \tag{9}$$

In the above formula, x_i represents the ith data before the vector normalization process, y_i represents the ith data after the normalization process, x_{max} refers to the maximum value of the data, and x_{min} refers to the minimum value of the data.

2.4 Dimensionality reduction

Assuming that there are n eigenvectors in total, and the optimal eigenvalues are selected from them, 2n-1 new features can be obtained. It should be noted that with the continuous increase of the number of features, the actual calculation will become more and more difficult, and in practical application, the number of features far exceeds the number of features measured by experiments, which will occupy a large number of computing and storage resources. After the feature dimensionality reduction process is completed, the feature subset selection algorithm is used to obtain a new feature space [12].

The principal component analysis algorithm can assume that the sample set is

$$D = \{x_1, x_2, \cdots, x_n\} \tag{10}$$

Get the new feature set as

$$C = [c_1, c_2, \cdots, c_l] \tag{11}$$

Each of these feature values, C_J, can represent a subset of the original features

$$U = [u_1, u_2, \cdots, u_m] \tag{12}$$

A linear combination of all features, and the following conditions are met:

$$c_i = a_{i1}u_1 + a_{i2}u_2 + \cdots + a_{im}u_m, \forall i \in \{1, \ldots, l\} \tag{13}$$

In the above formula, a_{ij} represents the content obtained from the characteristic values of the original space, and it is compliant

$$\sum_{j=1}^{m} a_{ij} = 1 \tag{14}$$

This requirement. Under the influence of the above formula, the feature with the largest difference in the combination is the first principal component. The relationship between two features can be accurately judged, so the selection of components that are not related to each other can effectively avoid the overlap of the extracted feature information. If all principal components are not correlated with each other, then the covariance is zero [13]. The actual calculation steps are as follows:

First, assuming that the sample size is n and the actual computing dimension is m, the original data is composed of n×m matrix.

Second, calculate the average value of all the values in the sample, subtract the average value from each row, then you can get a new matrix X_a, the sample is centralized, and the actual process is as follows:

$$x_i \leftarrow x_i - \frac{1}{n}\sum_{i=1}^{n} x_i \tag{15}$$

Third, the covariance matrix is calculated and analyzed

$$S = \frac{1}{m} X_a X_a^T \tag{16}$$

Define the characteristic values

and the corresponding eigenvectors;

$$\lambda_i(\lambda_1, \lambda_2, \cdots, \lambda_m) \tag{17}$$

Fourthly, the features are analyzed in the order from large to small, and the eigenvalues and their corresponding eigenvectors of the first k rows are obtained according to the cumulative contribution rate of variance, so as to form the matrix P, and the result is as follows:

$$\lambda_i(\lambda_1, \lambda_2, \cdots, \lambda_m) \tag{18}$$

Fifth, Y=PX is a completely new feature space.

When using the eigennumerical values to calculate the variance and contribution rate, the k value is selected, then the contribution rate formula of the k-th principal component Yk is as follows:

$$\omega_k = \lambda_k / \sum_{i=1}^{p} \lambda_i (k = 1,2, \cdots, p) \tag{19}$$

The formula for calculating the cumulative contribution of the first l principal components is as follows:

$$\psi_l = \sum_{i=1}^{l} \lambda_i / \sum_{i=1}^{m} \lambda_m \tag{20}$$

2.5 Feature subset selection algorithm

Principal component analysis projects a subset of the original features into a new feature space, removes the redundant correlation information between some features, reduces the use of memory space, and narrows the selection range of features after dimensionality reduction [14]. Due to the optimal feature subset can effectively achieve dimensionality reduction, there are two most commonly used methods, one is a filter and the other is a wrapper. Although the actual operation speed of the former is faster in the study of internal feature measurement, it is usually used for pretreatment, and there is an essential difference between experimental research and practical application. The latter will regard the accuracy and recognition rate of the classifier as the application standard for judging the subset of features, and the actual deviation is too small, but it is not suitable for the place with large feature latitude, so it can be organically combined with the component analysis method to operate, and the actual selection algorithm process is shown in Figure 4 below

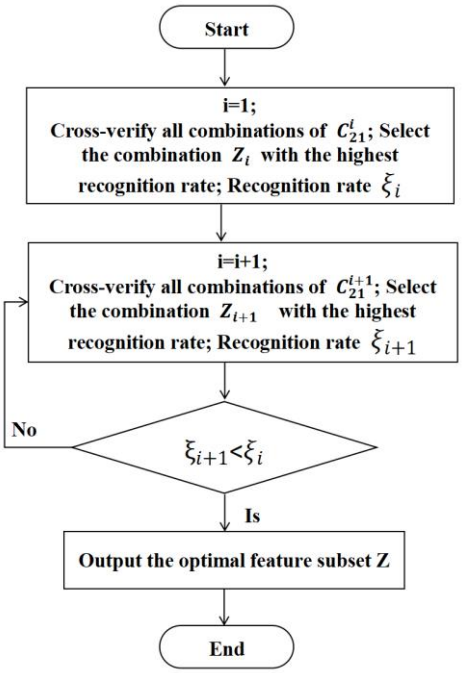

Figure 4 Flow chart of feature subset selection algorithm

3 Experimental analysis

In order to verify the performance of the above-mentioned Erhu performance posture correction system with wearable and body sensing technology as the core, the PC was selected as the laboratory desktop, the system was Windows 7, and the wireless human posture recognition system was used to obtain the human posture data of the experimenters, and in order to better understand the application performance of the algorithm, three experiments were conducted: first, starting from the initial position, the right arm was moved to the left by 10°, 20°, 30°, 40°, 50°, 60° accurately record the measured value of the left arm offset angle in different states; Secondly, starting from the initial position, the right arm moves up the same degree to accurately record the measured value of the

inclination angle in different states. Finally, starting from the initial position, the right arm rotates the same degree clockwise to accurately record the measured value of the rotation angle in different states, and the actual result is shown in Table 2 below

Table 2 Measurement results of offset angles

Measurement Angle α	True Value of φ(α)	Measured Value of φ'(α)
10°	10°	12.47°
20°	20°	20.25°
30°	30°	31.12°
40°	40°	312.81°
50°	50°	48.46°
60°	60°	512.121°

Table 3 Measurement results of inclination angle

Measurement Angle α	True Value of θ(α)	Measured Value of θ'(α)
10°	10°	10.31°
20°	20°	20.35°
30°	30°	212.31°
40°	40°	312.48°
50°	50°	50.61°
60°	60°	512.76°

Table 4 Measurement results of rotation angle

Measurement Angle α	True Value of γ(α)	Measured Value of γ'(α)
10°	10°	10.74°
20°	20°	20.13°
30°	30°	30.40°

40°	40°	40.56°
50°	50°	50.27°
60°	60°	60.45°

And the average error coefficient of the actual measurement is as follows:

$$\varepsilon_{\varphi} = \frac{\sum_{10}^{60} \frac{|\varphi(\alpha) - \varphi'(\alpha)|}{\varphi(\alpha)}}{6} = 0.025\varepsilon_{\theta} \tag{21}$$

$$\varepsilon_{\theta} = \frac{\sum_{10}^{60} \frac{|\theta(\alpha) - \theta'(\alpha)|}{\theta(\alpha)}}{6} = 0.017 \tag{22}$$

$$\varepsilon_{\gamma} = \frac{\sum_{10}^{60} \frac{|\gamma(\alpha) - \gamma'(\alpha)|}{\gamma(\alpha)}}{6} = 0.020 \tag{23}$$

In the experimental study, after the above comparative analysis, it is found that the comparison of the three coefficients is as follows:

$$\varepsilon_{\varphi} > \varepsilon_{\gamma} > \varepsilon_{\theta} \tag{24}$$

In the process of attitude calculation, the offset angle can only be calculated and analyzed using the velocity data obtained by the spirometer sensor alone, but in addition to the tilt angle and rotation angle, the acceleration data obtained by the accelerometer can also be used for analysis [15]. From the overall point of view, the average error coefficients of the offset angle, inclination angle and rotation angle are low, which proves that the system and the corresponding algorithm studied in this paper have high precision and can better obtain the change of human posture.

4 Conclusion

The gait correction system proposed in this study has shown significant advantages over traditional solutions in several important aspects. First of all, the system greatly improves the correction effect while ensuring the safety of users. This is mainly due to its advanced sensor technology and intelligent algorithms, which can accurately capture and analyze the user's gait data to provide tailor-made correction solutions. In addition, the systematic scientific correction ability is also a major feature. It not only identifies gait abnormalities, but also provides targeted training programs to help users gradually improve their gait and reduce the risk of physical discomfort and injury caused by gait problems. In summary, the gait correction system in this study has excellent performance in terms of safety, effectiveness, economy and applicability, which has brought innovation and progress to the field of gait correction, and has broad development prospects and application value. To sum up, compared with the traditional gait correction system, the research system in this paper is safer and

more effective, effectively controls the cost expenditure, scientifically corrects the user's gait, and the user can choose a variety of gait correction modes, and has a wider range of practical applications.

References

[1] Lu, L., Zhang, J., Xie, Y., Gao, F., Xu, S., Wu, X., & Ye, Z. (2020). Wearable health devices in health care: Narrative systematic review. JMIR mHealth and uHealth, 8(11), e18907.

[2] Wang, L. H., Ding, W. Q., & Sun, Y. G. (2022). Spinal ascending pathways for somatosensory information processing. Trends in Neurosciences, 45(8), 594-607.

[3] Dong, H., Yang, H., Ding, S., Li, T., & Yu, H. (2022). Bioinspired amphibious origami robot with body sensing for multimodal locomotion. Soft Robotics, 9(6), 1198-1209.

[4] Farr, D. E., Haddock, N. T., Tellez, J., Radi, I., Alterio, R., Sayers, B., & Zeh, H. (2024). Safety and feasibility of single-port robotic-assisted nipple-sparing mastectomy. JAMA Surgery, 159(3), 269-276.

[5] Chang, A. H., Rasmussen, S. Z., Jensen, A. E., Sørensen, T., & Rathleff, M. S. (2022). What do we actually know about a common cause of plantar heel pain? A scoping review of heel fat pad syndrome. Journal of Foot and Ankle Research, 15(1), 60.

[6] Chakraborty, S., & Rayalu, S. (2021). Detection of nickel by chemo and fluoro sensing technologies. Spectrochimica Acta Part A: Molecular and Biomolecular Spectroscopy, 245, 118915.

[7] Liu, F., Deswal, S., Christou, A., Sandamirskaya, Y., Kaboli, M., & Dahiya, R. (2022). Neuro-inspired electronic skin for robots. Science Robotics, 7(67), eabl7344.

[8] Gilday, K., Hughes, J., & Iida, F. (2023). Sensing, actuating, and interacting through passive body dynamics: A framework for soft robotic hand design. Soft Robotics, 10(1), 159-173.

[9] Rehan, M., Al-Bahadly, I., Thomas, D. G., Young, W., Cheng, L. K., & Avci, E. (2023). Smart capsules for sensing and sampling the gut: Status, challenges and prospects. Gut, 73(1), 186-202.

[10] Peng, Z., Iwabuchi, S., Izumi, K., Takiguchi, S., Yamaji, M., Fujita, S., Suzuki, H., Kambara, F., Fukasawa, G., Cooney, A., Di Michele, L., Elani, Y., Matsuura, T., & Kawano, R. (2024). Lipid vesicle-based molecular robots. Lab on a Chip, 24(5), 996-1029.

[11] Han, Y., Li, J., Chen, T., Gao, B., & Wang, H. (2023). Modern microelectronics and microfluidics on microneedles. The Analyst, 148(19), 4591-4615.

[12] Andreozzi, E., Esposito, D., & Bifulco, P. (2022). Contactless electrocatheter tracing within human body via magnetic sensing: A feasibility study. Sensors, 22(10), 3880.

[13] Carr, M., Haar, A., Amores, J., Lopes, P., Bernal, G., Vega, T., Rosello, O., Jain, A., & Maes, P. (2020). Dream engineering: Simulating worlds through sensory stimulation. Consciousness and Cognition, 83, 102955.

[14] Jeerapan, I., Moonla, C., Thavarungkul, P., & Kanatharana, P. (2022). Lab on a body for biomedical electrochemical sensing applications: The next generation of microfluidic devices. Progress in Molecular Biology and Translational Science, 187(1), 249-279.

[15] Chen, K., Yang, H., & Cai, R. (2025). Microfluidics for nanomedicine delivery. ACS Biomaterials Science & Engineering, 11(2), 774-783.

About the Author

Yubo Wang was born in YunNan, China, in 1986. From 2005 to 2009, she studied in Shool of music of Minzu University of China and received his bachelor's degree in 2009. From 2013 to 2017, she studied in Art College of JiLin University and received his Master’s degree in 2017. From 2022 to 2025, she studied in SHINAWATRA University and received her Doctor's of Philosophy degree in early 2025. She has been working at Zhuhai College of Science and Technology since 2009. Her research interests are included Her research interests include erhu performance and music theory research.